

# The Long Non-Coding RNA *HOTAIR* Is a Critical Epigenetic Mediator of Angiogenesis in Diabetic Retinopathy

Saumik Biswas,<sup>1</sup> Biao Feng,<sup>1</sup> Shali Chen,<sup>1</sup> Jieting Liu,<sup>1</sup> Erfan Aref-Eshghi,<sup>1</sup> John Gonder,<sup>2</sup> Vy Ngo,<sup>1</sup> Bekim Sadikovic,<sup>1</sup> and Subrata Chakrabarti<sup>1</sup>

<sup>1</sup>Department of Pathology and Laboratory Medicine, Western University, London, Ontario, Canada

<sup>2</sup>Department of Ophthalmology, Western University, London, Ontario, Canada

Correspondence: Subrata Chakrabarti, Department of Pathology and Laboratory Medicine, Western University, DSB 4033, 1151 Richmond Street, London, Ontario, N6A 5C1, Canada; [subrata.chakrabarti@lhsc.on.ca](mailto:subrata.chakrabarti@lhsc.on.ca)

**Received:** November 12, 2020

**Accepted:** February 15, 2021

**Published:** March 16, 2021

Citation: Biswas S, Feng B, Chen S, et al. The long non-coding RNA *HOTAIR* is a critical epigenetic mediator of angiogenesis in diabetic retinopathy. *Invest Ophthalmol Vis Sci.* 2021;62(3):20. <https://doi.org/10.1167/iovs.62.3.20>

**PURPOSE.** Diabetic retinopathy (DR) remains a pressing issue worldwide. Abnormal angiogenesis is a distinct vascular lesion in DR, and research has established that vascular endothelial growth factor A (VEGF-A) is a primary mediator of such changes. However, limitations in current anti-VEGF therapies suggest that our understanding of molecular networks underlying ocular angiogenesis remains far from complete. Based on our long non-coding RNA (lncRNA) array analyses, HOX antisense intergenic RNA (*HOTAIR*) was identified as one of the top upregulated lncRNAs in high glucose-cultured human retinal endothelial cells (HRECs). Given the well-documented roles of *HOTAIR* in cancer, no studies have examined the epigenetic implications of *HOTAIR* in DR, and we investigated such relationships herein.

**METHODS.** We used HRECs exposed to various glucose concentrations and epigenetic modulators to examine *HOTAIR*, angiogenic, and DR-related molecular markers. Oxidative stress, angiogenesis, and mitochondrial dysfunction were assessed. Retinal tissues of diabetic rodents and the vitreous humor and serum of patients with proliferative DR were also investigated.

**RESULTS.** Hyperglycemia significantly augmented *HOTAIR* expression in HRECs and promoted angiogenesis, oxidative damage, and mitochondrial aberrations. Similarly, vitreous humor and serum from proliferative DR patients and retinas from diabetic animals demonstrated increased *HOTAIR* expression compared to non-diabetic controls. *HOTAIR* knockdown protected against glucose-induced increases of angiogenic and diabetes-associated molecules in the retina. Mechanistically, we showed that *HOTAIR* exerts its capabilities by preventing oxidative stress and modulating epigenetic pathways involving histone methylation, histone acetylation, DNA methylation, and transcription factors.

**CONCLUSIONS.** Our findings suggest that *HOTAIR* is a critical lncRNA in the pathogenesis of DR and may potentially be important for diagnostic and therapeutic targeting.

**Keywords:** lncRNA, *HOTAIR*, epigenetics, angiogenesis, diabetic retinopathy

With diabetes mellitus (DM) projected to impact over 600 million people globally in the next 20 years,<sup>1</sup> the risks of micro- and macrovascular complications remain a serious concern. Hyperglycemia in DM alters biochemical and metabolic pathways, contributing to vascular damage in chronic complications.<sup>2</sup> In this study, we investigated diabetic retinopathy (DR), which is a debilitating microvascular complication and a major cause of blindness worldwide.<sup>3</sup> DR can be categorized as non-proliferative DR and proliferative DR (PDR), the latter manifesting as pathological neovascularization.<sup>1-3</sup>

In PDR, angiogenesis occurs due to the activation of various signaling cascades that promote increased levels of angiogenic factors.<sup>4</sup> These factors mediate the proliferation of retinal endothelial cells (ECs), leading to abnormal neovascularisation.<sup>3</sup> Vascular endothelial growth factor (VEGF) is a potent angiogenic factor expressed by ECs

and non-ECs, and several pathological processes, including hypoxia,<sup>5</sup> oxidative stress,<sup>6</sup> and inflammation,<sup>7</sup> stimulate VEGF expression through transcriptional regulation, including non-coding RNAs.<sup>2,8,9</sup> Due to the critical role of VEGF, the first-line therapy for patients with diabetic macular edema (DME) and PDR consists of intravitreal injections of anti-VEGF. However, such therapies have limitations where frequent intraocular injections are required and have local or systemic adverse effects.<sup>10</sup> Furthermore, patients with DME can be unresponsive to anti-VEGF treatments.<sup>10,11</sup> Hence, new studies are warranted to identify novel therapeutic targets.

Recently, genomic technologies have identified long non-coding RNAs (lncRNAs), which are larger than 200 base-pairs and possess limited protein-coding capacities. lncRNAs are dynamically regulated and have distinct functionalities facilitating chromatin remodeling, and they help govern

the expression of genes involved in biological processes, including DR.<sup>12–14</sup> However, detailed characterization of the functions of certain lncRNAs in DR is lacking.

We initially carried out a lncRNA microarray using human retinal endothelial cells (HRECs; GEO ID: 122189), and such analyses demonstrated a glucose-induced increase in HOX antisense intergenic RNA (*HOTAIR*) expression by 2.7-fold. Therefore, in this research, we directed our efforts toward thoroughly characterizing the epigenetic implications of *HOTAIR* in DR. Using both in vitro and in vivo models, we confirmed glucose-induced increases of *HOTAIR* and demonstrated its role in angiogenesis and glucose-induced mitochondrial and DNA damage through related epigenetic pathways.

## METHODS

### Cell Culture

HRECs (Cell Systems, Kirkland, WA, USA) and mouse retinal microvascular endothelial cells (Applied Biological Materials, Richmond, BC, Canada) were cultured in Endothelial Basal Medium-2 (Lonza, Walkersville, MD, USA), as described previously, and were used between passages 3 and 6 (see Supplementary Materials).<sup>9,13,14</sup> At 80% confluence, ECs were cultured in serum-free medium overnight before exposure to various D-glucose levels, epigenetic blockers, or siRNA treatments. All in vitro or ex vivo experiments were independently repeated at least three times and performed with six replicates, unless specified.

### Endothelial Tube Formation Assay

Approximately  $1.5 \times 10^4$  HRECs were used, as described (see Supplementary Materials).<sup>9,14</sup> Images were captured at 6 hours ( $n = 8$  independent samples per group). The total number of tubules and branching points was assessed using WimTube Image analyzer software (Wimasis, Córdoba, Spain).

### RNA Fluorescence In Situ Hybridization

RNA fluorescence in situ hybridization (FISH) was performed, as described (see Supplementary Materials),<sup>9</sup> using Stellaris FISH Probes, Human *HOTAIR*, with Quasar 570 Dye (5 nmol; Biosearch Technologies, Petaluma, CA, USA).

### JC-1 and 8-OHdG Staining

HRECs were stained with 10  $\mu$ M of JC-1 dye (Abcam, Cambridge, UK), 4',6-diamidino-2-phenylindole (DAPI), or 8-hydroxy-2'-deoxyguanosine (8-OHdG, 1:50; Santa Cruz Biotechnology, Dallas, TX, USA) counterstains following the manufacturer's instructions. Images were captured using the Zeiss LSM 410 inverted laser-scanning microscope (Carl Zeiss, Wetzlar, Germany) and were analyzed using ImageJ (National Institutes of Health, Bethesda, MD, USA) (see Supplementary Materials).<sup>15</sup>

### Animal Models

The Western University Council for Animal Care Committee approved all animal experiments, which were performed in accordance with the ARVO Statement for the Use of Animals

in Ophthalmic and Vision Research. As our previous studies were performed in male mice, we selected only male rats (Sprague–Dawley;  $174.9 \pm 2.96$  g; 6 weeks old) and mice (C57/BL6J background;  $25.7 \pm 1.82$  g; 8 weeks old) (Charles River Laboratories, Wilmington, MA, USA) for our study and randomly divided them into control and diabetic groups. Streptozotocin (STZ) was used to generate a type 1 diabetic animal model. Animal monitoring and tissue collection have been described previously.<sup>9,13</sup>

For the therapeutic in vivo model (4-week duration), mice (with or without diabetes) were randomly divided into four groups ( $n = 6$ /group). Intravitreal injections of scrambled (SCR) siRNA or siHOTAIR (1  $\mu$ L of 100 nmol/L in Invitrogen Lipofectamine 2000; Thermo Fisher Scientific, Waltham, MA, USA) following isoflurane anesthesia were administered once every week for 3 weeks using a 33-gauge needle as described previously.<sup>17</sup> Also, to circumvent inflammation and damage from the intravitreal procedure, external regions of the injected eye were immediately treated with a single drop of proparacaine hydrochloride ophthalmic solution (0.5%; Alcon, Geneva, Switzerland) and neomycin and polymyxin B sulfates and bacitracin ophthalmic ointment (Vétoquinol Canada, Lavaltrie, QC, Canada). Toxicity analyses were done after the single injections (see Supplementary Materials).

### Clinical Samples

The Western Research Ethics Board at the University of Western Ontario approved this study. Patients provided informed consent prior to the procedure and all samples were handled in accordance with the tenets of the Declaration of Helsinki. Both serum and vitreous humor (VH) were collected from patients undergoing a pars plana vitrectomy (Supplementary Table S3). Specimens were categorized into two groups: control and PDR. Mean age of PDR group was  $60.9 \pm 10.43$  years ( $n = 11$ ; 10 males, one female) and that of the (non-diabetic) control group was  $69.2 \pm 8.87$  years ( $n = 10$ ; two males, eight females). RNA extraction and quantitative reverse transcription PCR (RT-qPCR) assays are described in the Supplementary Materials.

### Methylation Analysis of CpG Sites Across *HOTAIR*

Methylation patterns of CpG sites across the *HOTAIR* gene were examined in HRECs using the Illumina Infinium MethylationEPIC BeadChip array (Illumina, Inc., San Diego, CA, USA), following the manufacturer's instructions and our previously published protocols (see Supplementary Materials).<sup>16</sup>

### Statistical Analyses

Data are presented as mean  $\pm$  SEM or mean  $\pm$  SD. Experiments were performed in triplicate ( $n = 6$ /group), unless specified otherwise. Statistical significance ( $P < 0.05$ ) was assessed by the Mann–Whitney *U* test or Student's *t*-test or one-way ANOVA, followed by Tukey's post hoc test, as appropriate.

### Data and Resource Availability

All data generated or analyzed during this study are included in this published article and its Supplementary Materials.

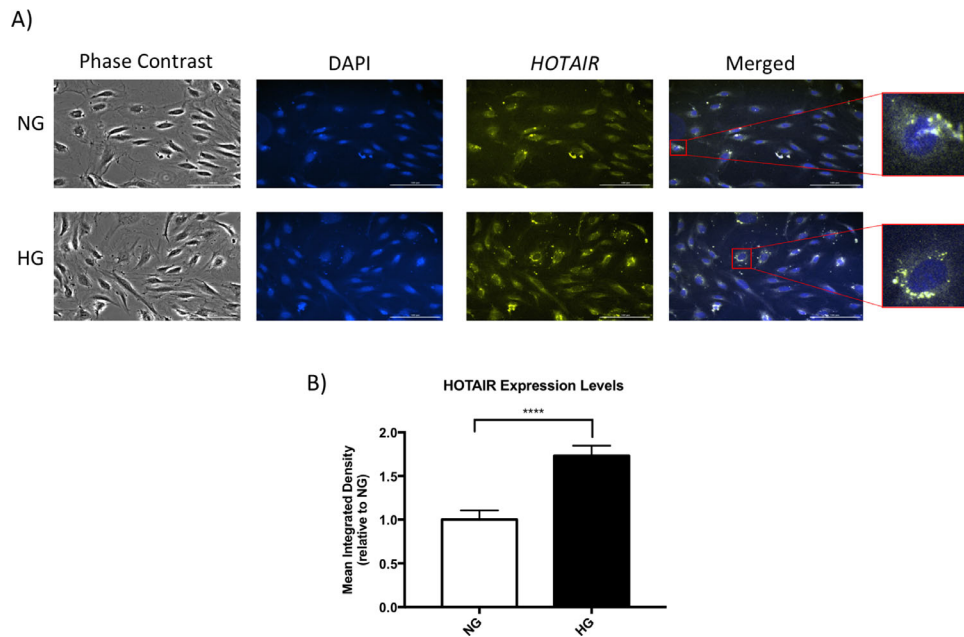


**FIGURE 1.** *HOTAIR* is localized in the nucleus and cytoplasm of retinal endothelial cells. (A) *HOTAIR* localization in HRECs at 48 hours as indicated by RNA FISH using Stellaris FISH probes for human *HOTAIR*. Cells were also counterstained with DAPI to visualize the nuclei. The upper panel inset demonstrates nuclear localization of *HOTAIR*, and the lower panel inset demonstrates perinuclear localization. Original magnification, 20 $\times$ . Scale bars: 100  $\mu$ m. (B) Mean integrated densities of *HOTAIR* expression calculated using ImageJ (normalized to NG). Statistical significance was assessed using two-tailed Student's *t*-test (\*\*\*\**P* < 0.0001). Data represent the mean  $\pm$  SEM of 50 cells captured per sample (*n* = 4 or 5 independent samples per group).

## RESULTS

### *HOTAIR* RNA Expression Is Glucose Dependent

In our array analyses (GEO ID: 122189) and following stringent filtering criteria (fold change  $\leq 2$  or  $\geq 2$ ), 2669 to 3518 lncRNAs were upregulated and 890 to 1991 lncRNAs were downregulated in high glucose (HG) (Supplementary Figs. S1A–C). RT-qPCR confirmed the glucose-induced expression of *HOTAIR* (Supplementary Fig. S2A), along with augmented expression of *VEGF-A* and *ET-1* transcripts (Supplementary Figs. S2B, C). We also investigated *HOTAIR* expression at different time points with various glucose levels. *HOTAIR* demonstrated significant HG-induced elevations at 48 hours (*P* = 0.0014). Hence, the 48-hour time point was used for subsequent experiments. No significant differences in *HOTAIR*, *VEGF-A*, or *ET-1* expression were observed in osmotic controls (25-mM L-glucose) (Supplementary Fig. S2). RNA FISH was used to delineate the subcellular localization of *HOTAIR*. *HOTAIR* was present in both the nucleus and perinuclear/cytoplasmic regions (Fig. 1A). Furthermore, HG significantly elevated the expression of *HOTAIR* (Fig. 1B). These findings suggest that *HOTAIR* may be implicated in both nuclear and cytoplasmic processes.

### *HOTAIR* Knockdown Prevents Glucose-Mediated Induction of Multiple Angiogenic Factors, Epigenetic Mediators, and EC Dysfunction-Related Molecules

Based on our findings, we explored additional angiogenic factors,<sup>18</sup> including angiopoietin-like 4 (ANGPTL4), placental growth factor (PGF), hypoxia-inducible factor (HIF),

interleukin-1 beta (IL-1 $\beta$ ), as well as epigenetic mediators and EC damage-induced molecules, including poly(ADP-ribose) polymerase 1 (PARP1)<sup>19</sup> and cytochrome *b*, by performing loss-of-function studies using siRNA-mediated knockdown of *HOTAIR*. Significantly decreased *HOTAIR* expression was observed across all siRNA transfections, with SMARTpool siHOTAIR showing the largest reduction of *HOTAIR* RNA levels (~91%) (Supplementary Fig. S3). Hence, we selected SMARTpool siRNA for subsequent analyses.

siHOTAIR-transfected HRECs in HG showed decreased expression of multiple RNA transcripts implicated in angiogenesis (*VEGF-A*, *ET-1*, *ANGPTL4*, *PGF*, *HIF-1 $\alpha$* ) (Fig. 2); DNA and oxidative damage (*PARP-1* and *cytochrome b*) (Fig. 2); and epigenetic regulation (*EZH2*, *SUZ12*, *DNMT1*, *DNMT3A*, *DNMT3B*, *CTCF*, and *P300*) (Supplementary Fig. S4), compared to SCR siRNA-transfected cells in HG. To determine whether these changes are reflected at the protein level, we performed ELISAs for the most characterized angiogenic markers, VEGF-A and HIF-1 $\alpha$ . As expected, *HOTAIR* knockdown prevented glucose-induced upregulation of VEGF-A and HIF-1 $\alpha$  proteins (Supplementary Figs. S5A, B). We additionally examined the RNA expression of *HOXD3* and *HOXD10*, because *HOTAIR* transcriptionally represses *HOXD*.<sup>20</sup> Knockdown of *HOTAIR* in HG induced upregulation of *HOXD3* and *HOXD10*, compared to SCR HG (Supplementary Figs. S5C, D). We also investigated the viability of HRECs following siHOTAIR treatment and showed that *HOTAIR* siRNA transfection did not cause increased cell death but instead improved cellular viability compared to SCR controls (Supplementary Fig. S5E). These results suggest that *HOTAIR* is a possible epigenetic regulator of glucose-induced EC dysfunction and angiogenesis.



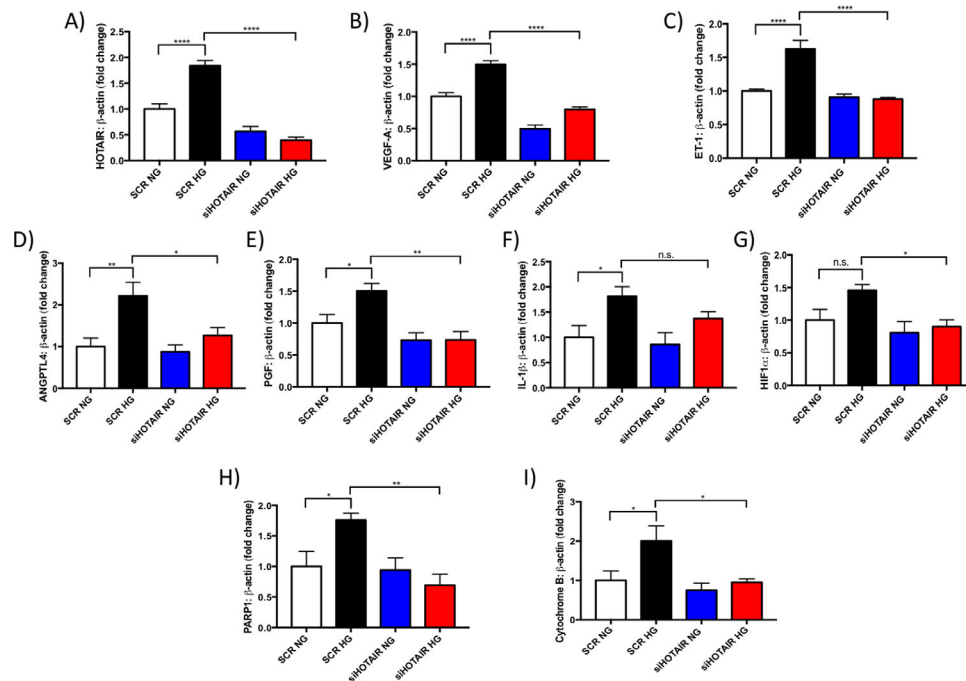


**FIGURE 2.** *HOTAIR* knockdown prevents glucose-mediated induction of several angiogenic factors and diabetes-related molecules in vitro. RT-qPCR analyses of expression of (A) *HOTAIR*, (B) *VEGF-A*, (C) *ET-1*, (D) *ANGPTL4*, (E) *PGF*, (F) *IL-1β*, (G) *HIF-1α*, (H) *PARP1*, and (I) *cytchrome b* following the administration of SCR siRNA or siHOTAIR in HRECs subjected to 48 hours of NG or HG culture. Data are expressed as a ratio to  $\beta$ -actin and normalized to SCR NG. Statistical significance was assessed using one-way ANOVA for multiple comparisons, followed by Tukey's post hoc test (\* $P < 0.05$ , \*\* $P < 0.01$ , \*\*\* $P < 0.001$ , \*\*\*\* $P < 0.0001$ ; n.s., not significant). Data represent the mean  $\pm$  SEM of three independent experiments ( $n = 6$ /group).

### ***HOTAIR* Mediates Angiogenesis In Vitro**

To examine the role of *HOTAIR* in angiogenesis in hyperglycemia, we used a tube formation assay.<sup>21</sup> At 6 hours, cells transfected with SCR in HG showed increased capillary tubules compared to SCR-transfected cells in normoglycemia (NG) (Fig. 3). Following siHOTAIR transfection, the degree of branching and total number of tubules were decreased in both NG and HG (Figs. 3B, C). Interestingly, following siHOTAIR transfection, exogenous VEGF proteins were unable to recover HG-induced changes, implying that *HOTAIR* knockdown may be further desensitizing ECs to additional angiogenic factors.

### **Diabetic Rodents Show Increased Retinal *HOTAIR* Levels**

We then examined *HOTAIR* in the retina during diabetes. We used both STZ-induced diabetic mice and rats after 2 months of diabetes. Diabetic animals showed hyperglycemia, glucosuria, and reduced body weight (not shown). Significant upregulation of *HOTAIR* in the retinas of both diabetic mice and rats was observed at 2 months (Supplementary Figs. S6A, B). To evaluate the therapeutic potential of *HOTAIR*, we used a SMARTpool siHOTAIR that specifically targeted mouse *HOTAIR*. In mouse retinal microvascular endothelial cells in HG, 50 nM and 100 nM of siHOTAIR evoked significant reductions (~79% and ~80%, respectively) of *HOTAIR* RNA, as well as *VEGF-A* and *ANGPTL4* transcripts (at 100-nM concentration) (Supplementary Figs. S7A–C).

### **Intravitreal Injections of siHOTAIR Prevent Early DR-Related Retinal Changes and Diabetes-Induced Retinal Vascular Permeability**

We initially performed a toxicology study involving siHOTAIR. Wild-type C57BL/6J mice were subjected to a one-time intravitreal injection of either SCR siRNA (100 nM) or siHOTAIR at varying concentrations (25, 50, or 100 nM) and were monitored for 7 days when tissues were collected. After 7 days, retinal *HOTAIR* expression appeared to be the lowest following a 100-nM dose of siHOTAIR (~50% reduction) when compared to SCR controls (Supplementary Fig. S8A). No behavioral changes were observed, and analysis of H&E stained sections showed no structural abnormalities across retinal, heart, lung, liver, or kidney tissues (Supplementary Figs. S8B–F). Hence, for therapeutic assessment, 100 nM of siHOTAIR or SCR was intravitreally injected weekly in diabetic mice showing hyperglycemia and loss of body weight (Supplementary Figs. S9A, B), and *HOTAIR* knockdown did not affect these parameters. However, at 4 weeks, elevated RNA expression of *HOTAIR*, *Vegf-a*, *Ctcf*, *Et-1*, *Angptl4*, *Mcp-1*, *Il-1β*, *Pgf*, *Hif-1α*, *p300*, polycomb repressive complex 2 (*Prc2*) components (*Ezh2*, *Suz12*, and *Eed*), *Hoxd3*, and *Parp1* were seen in the retina of diabetic mice administered SCR siRNAs (Fig. 4; Supplementary Figs. S9C–I). Knockdown of *HOTAIR* (~58% reduction) reduced diabetes-induced upregulations of most of these transcripts, suggesting that *HOTAIR* knockdown protects against early diabetes-induced molecular aberrations in the retina. However, we did not observe differences in retinal expression of *Il-1β*, *Pgf*, and *Hoxd3* between

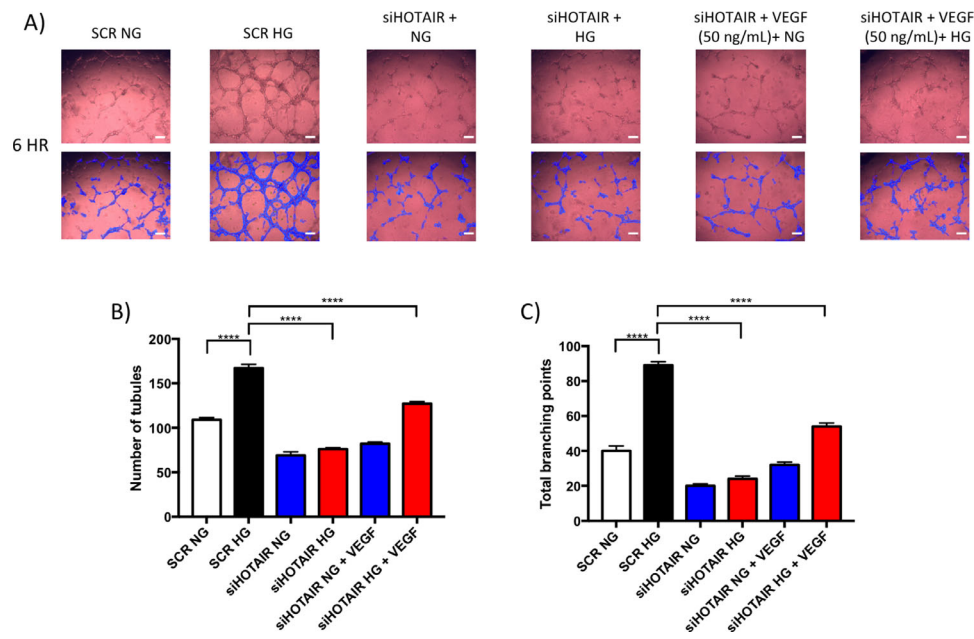


**FIGURE 3.** *HOTAIR* mediates angiogenesis in vitro. (A) Endothelial tube formation assay at the 6-hour mark for HRECs treated with scrambled (SCR) siRNA, siHOTAIR, or exogenous VEGF and cultured in NG or HG conditions. WimTube Image analyzer software was used to calculate (B) the number of tubules and (C) the total branching points in each group. Glucose-induced angiogenesis was prevented by siHOTAIR, but only partially reversed by VEGF supplementation. Statistical significance was assessed using one-way ANOVA for multiple comparisons, followed by Tukey's post hoc test (\*\*\*\* $P < 0.0001$ ). Data represent the mean  $\pm$  SEM of three independent experiments ( $n = 8$ /group), and images were captured from at least two field views per well (original magnification,  $40\times$ ).

SCR and siHOTAIR-treated animals (Figs. 4G; Supplementary Figs. S9F, I). Retinal vascular permeability was also assessed by immunohistochemical staining for immunoglobulin G (IgG). Our findings demonstrated that IgG was mainly localized within the capillaries, without any significant staining of retinal tissues in non-diabetic animals treated with SCR or *HOTAIR* siRNAs (Fig. 4I, score 1). Conversely, diffuse extravascular IgG staining was observed in the retinal tissues of diabetic animals treated with SCR siRNAs, signifying increased extravasation in the neural retina (Fig. 4J, score 3), whereas *HOTAIR* knockdown protected diabetic animals from such changes (Fig. 4L, score 1).

We further measured retinal VEGF-A proteins. VEGF-A was increased in the retinas of diabetic mice treated with SCR siRNAs, but siHOTAIR reduced retinal VEGF-A proteins in diabetic mice (Supplementary Fig. S9J). Moreover, we did not find any observable toxic effects in retinal, cardiac, lung, liver, kidney, and brain tissues following 1 month of siHOTAIR injections (Supplementary Fig. S10).

### ***HOTAIR* Is Upregulated in the Vitreous and Serum of Patients With PDR**

To determine the role of *HOTAIR* as a potential biomarker, we examined *HOTAIR* expression in the serum and VH of patients with PDR. *HOTAIR* expression was significantly upregulated in both vitreous and serum of patients with PDR compared to that of non-diabetic patients (Supplementary Fig. S11). A positive correlation for *HOTAIR* levels between serum and vitreous samples ( $R^2 = 0.482$ ) (Supplementary Fig. S11C) was seen, suggesting that *HOTAIR* may have potential to serve as a biomarker for DR.

### ***HOTAIR* Knockdown Prevents Glucose-Induced DNA and Mitochondrial Damage and Endothelial Cell Junction Disruptions**

To understand molecular mechanisms for *HOTAIR* and its role in mitochondrial dysfunction,<sup>22</sup> we assessed the mitochondrial transmembrane potential ( $\Delta\Psi$ M) in HRECs after *HOTAIR* knockdown by detecting JC-1 signals. HG significantly evoked mitochondrial depolarization compared to SCR NG controls (Fig. 5), whereas the knockdown of *HOTAIR* in NG increased mitochondrial activity. Interestingly, *HOTAIR* knockdown partially reduced HG-induced mitochondrial dysfunction/depolarization when compared to SCR HG.

As HG induces abnormalities in several metabolic pathways causing oxidative DNA damage,<sup>2</sup> we examined such relationships using 8-OHdG levels (a biomarker for oxidative DNA damage).<sup>15</sup> In comparison to SCR NG, SCR HG cells demonstrated increased 8-OHdG. Conversely, *HOTAIR* knockdown reduced glucose-induced increases in 8-OHdG expression (Fig. 6). Furthermore, the loss of endothelial junctions<sup>2</sup> was investigated electronmicroscopically. HG-induced disruptions of EC junctions were prevented by *HOTAIR* knockdown (Supplementary Fig. S12). Collectively, these results suggest that *HOTAIR* contributes to oxidative stress and EC dysfunction in DR.

### ***HOTAIR*-Induced Production of DR-Related Molecules Depends on Glycolytic Metabolism**

To delineate the regulatory mechanisms, we employed 2-deoxy-D-glucose (2-DG, a glycolytic pathway inhibitor<sup>23</sup>).

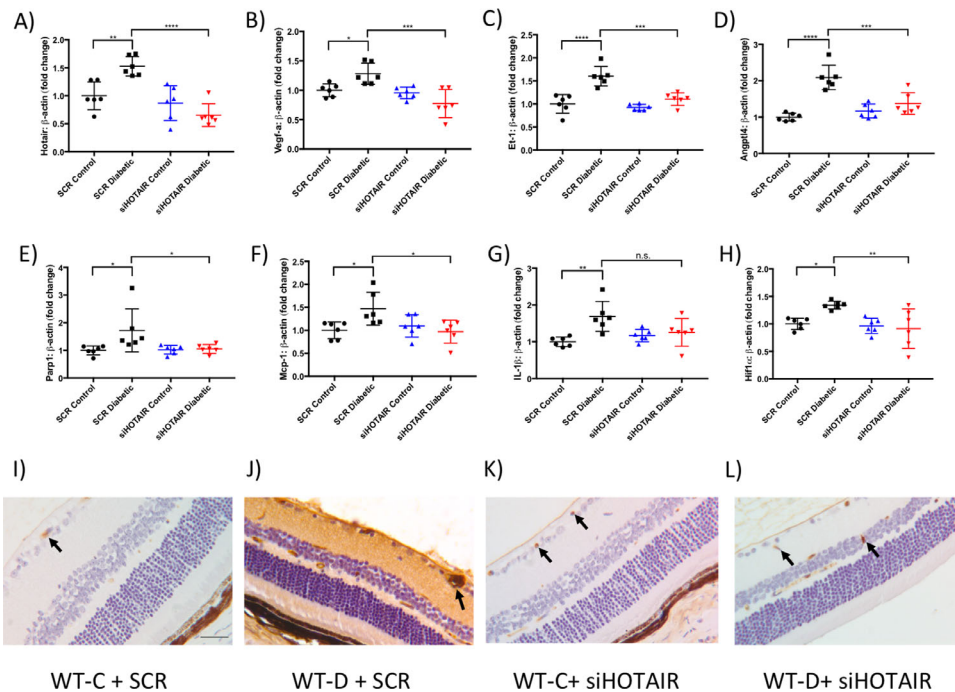


**FIGURE 4.** Knockdown of *HOTAIR* through intravitreal injections significantly prevents diabetes-induced retinal vascular permeability and early elevations of angiogenic and other molecules in the retina. RT-qPCR analyses of expression of (A) *HOTAIR*, (B) *Vegf-a*, (C) *Et-1*, (D) *Angptl4*, (E) *Parp1*, (F) *Mcp-1*, (G) *Il-1β*, and (H) *Hif-1α* in retinal tissues. Data are expressed as a ratio to  $\beta$ -actin and normalized to SCR control. Statistical significance was assessed using one-way ANOVA for multiple comparisons, followed by Tukey's post hoc test (\* $P < 0.05$ , \*\* $P < 0.01$ , \*\*\* $P < 0.001$ , \*\*\*\* $P < 0.0001$ ; n.s., not significant). Data represent the mean  $\pm$  SD ( $n = 6$ /group). Immunohistochemical staining of the mouse retina for IgG showed enhanced extravascular diffuse retinal stain, signifying increased extravasation in the diabetic mice with SCR siRNA (score = 3) (J) compared to non-diabetic controls with SCR siRNA (score = 1) (I). Photomicrographs for non-diabetic control mice (K) and diabetic mice administered siHOTAIR injections (L) showed positive IgG stains (arrows; score = 1) limited to the intravascular space. No changes in IgG leakage were demonstrated between control mice treated with SCR siRNA (I) and control mice treated with siHOTAIR (K). WT-C, wild-type non-diabetic control; WT-D, wild-type diabetic control; SCR, scrambled siRNA; siHOTAIR, siRNA targeting mouse *HOTAIR*. Original magnification, 200 $\times$  (I to L).

Accordingly, 2-DG treatment significantly blocked HG-induced expression of *HOTAIR* and its downstream molecules, *VEGF-A*, *ET-1*, *ANGPTL4*, *MCP-1*, *IL-1β*, *CTCF*, and *cytochrome b* (Supplementary Fig. S13). Furthermore, 2-DG evoked reductions in epigenetic molecules including *EZH2*, *SUZ12*, *EED*, and *DNMT1*, but not *DNMT3A* or *DNMT3B* (Supplementary Fig. S14). Interestingly, even at a 5-mM concentration, 2-DG treatments did not reduce *PARP1* and *P300* expression and did not augment *cytochrome b* expression, suggesting that there may be additional non-mitochondrial mechanisms leading to oxidative stress.<sup>24</sup> However, additional studies are needed to establish such a notion. Moreover, *HOXD3* and *HOXD10* expression was upregulated in 2-DG-treated HRECs in HG (Supplementary Figs. S14H, D), highlighting the inverse relationship between *HOTAIR* and *HOXD* expression. In keeping with a previous study that confirms the antiangiogenic activity of 2-DG,<sup>25</sup> our findings indicate that glucose works upstream of *HOTAIR* and causes cellular damage through both glycolysis and direct oxidative stress.

### Histone Methylation Regulates *HOTAIR* and Its Downstream Targets

As *HOTAIR* and PRC2 (a histone methyltransferase) may share a relationship,<sup>26</sup> we investigated histone methylation using a global histone methylation inhibitor, 3-

deazaneplanocin A (DZNep).<sup>27</sup> DZNep reduced glucose-induced increases of PRC2 components: *EZH2*, *SUZ12*, and *EED* transcripts (Supplementary Figs. S15A–C). Significant reductions following DZNep treatment of HG cells were also evident for *HOTAIR*, *VEGF-A*, *ANGPTL4*, *CTCF*, *PARP1*, *P300*, and *cytochrome b* transcripts (Supplementary Fig. S16). DZNep pretreatment, however, augmented the expression of *ET-1*, *MCP-1*, *IL-1β*, *HOXD3*, and *HOXD10* transcripts (Supplementary Figs. S15, S16). These observations, as seen before,<sup>9,14</sup> suggest that DZNep-mediated methylation blockade disrupts cellular cross-talk in ECs in HG.

To confirm these findings, we targeted *EZH2* (catalytic subunit of PRC2)<sup>28</sup> and *CTCF* (transcription factor maintaining chromosome organization and regulating *HOTAIR*)<sup>29</sup> for knockdown. Following siRNA transfections, significant reductions of *EZH2* and *CTCF* were observed (Supplementary Figs. S17E, F). *EZH2* inhibition reduced *HOTAIR*, *VEGF-A*, *ET-1*, *ANGPTL4*, *CTCF*, *SUZ12*, *PARP1*, *MCP-1*, *IL-1β*, *cytochrome b*, and *DNMT1* RNA expression and increased *P300*, *HOXD3*, and *HOXD10* transcript levels (Supplementary Figs. S17, S18). No differences in expression were observed for *DNMT3A* and *DNMT3B* following siEZH2 transfection. These findings imply that *EZH2* is directly involved in the transcriptional regulation of *HOTAIR* and several other downstream genes in hyperglycemia.

Knockdown of *CTCF* in HG-cultured HRECs produced differential expression of several genes, including significant increases in *HOTAIR*, *ANGPTL4*, *EED*, *IL-1β*, *Cytochrome B*,



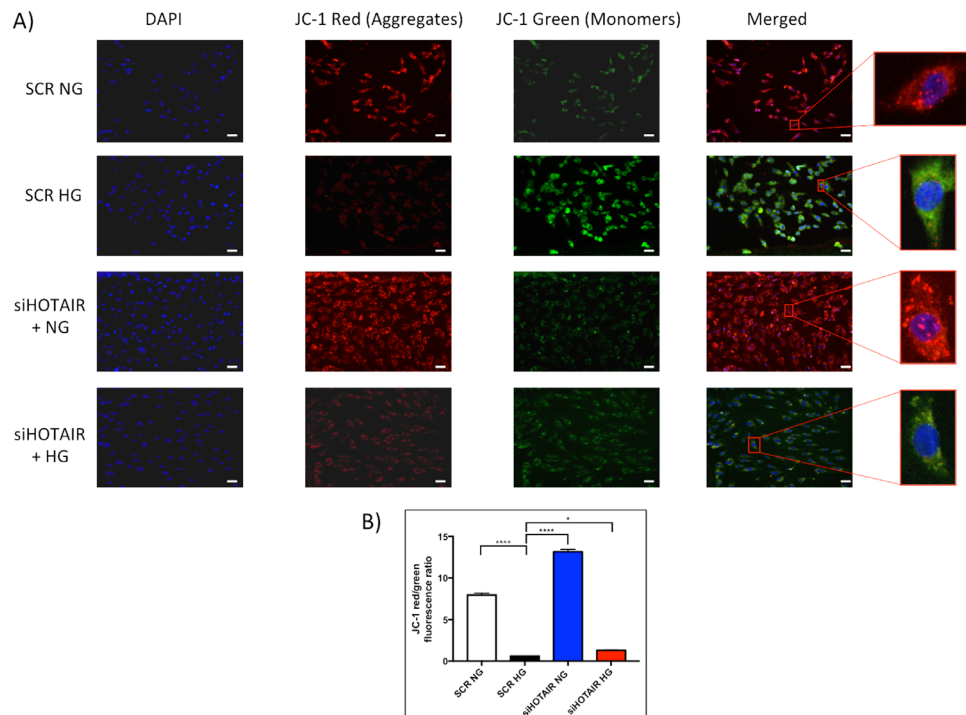


**FIGURE 5.** *HOTAIR* knockdown partially prevents glucose-induced mitochondrial depolarization/dysfunction. **(A)** Images captured from the JC-1 assay, where HRECs were pretreated with SCR siRNAs or siHOTAIR and subsequently cultured in NG or HG for 48 hours. JC-1 stains demonstrated HG-induced mitochondrial dysfunction (evidenced by low  $\Delta\Psi_m$  and more green and less red fluorescence when compared to SCR NG) and were partially corrected by *HOTAIR* knockdown (siHOTAIR). Cells were also counterstained with DAPI. Original magnification, 20 $\times$ . Scale bars: 100  $\mu$ m. **(B)** The JC-1 red/green fluorescence ratio was quantified using ImageJ. Statistical significance was assessed using one-way ANOVA for multiple comparisons, followed by Tukey's post hoc test (\* $P < 0.05$ , \*\* $P < 0.01$ , \*\*\* $P < 0.001$ , \*\*\*\* $P < 0.0001$ ; n.s., not significant). Data represent the mean  $\pm$  SEM of 20 cells captured per sample ( $n = 8$  independent samples per group).

*HOXD3*, and *HOXD10* and decreases in *ET-1*, *EZH2*, *PARP1*, *MCP-1*, *DNMT1*, and *P300* transcripts, compared to SCR HG cells. No differences were observed for *VEGF-A*, *SUZ12*, *DNMT3A*, and *DNMT3B* transcripts following *CTCF* transfection in HG-cultured HRECs (Supplementary Figs. S17, S18). These results suggest diverse roles of *CTCF* in gene regulation; for example, depletion of *CTCF* may augment glucose-induced gene expression, possibly through the inability of *CTCF* to block interactions between enhancers and promoters, or repress gene expression, possibly through chromatin architectural changes.<sup>30</sup>

### **HOTAIR Regulates VEGF by Binding With Histone-Modifying Enzymes**

To examine direct relationships between *HOTAIR* and histone-modifying enzymes, we performed a RNA immunoprecipitation assay. In comparison to IgG controls, *HOTAIR* RNA levels were enriched in the precipitated anti-EZH2 and P300-antibody fractions obtained from HRECs in HG (Supplementary Fig. S19), suggesting that HG promotes *HOTAIR* binding associations to EZH2 and P300. We also performed chromatin immunoprecipitation qPCR using antibodies for RNA polymerase II (indicative of transcriptional activity), H3K27me3 (indicative of transcriptional repression), and pan-H3K9/14/18/23/27 acetylation (indicative of transcriptional activation) and employed primers spanning the proximal and distal promoter regions of *VEGF-A*. Compared to NG, RNA polymerase II levels were signifi-

cantly enriched in both distal and proximal promoter regions of *VEGF-A* in HG (Supplementary Figs. S20A, D), which were prevented by *HOTAIR* knockdown. Conversely, HG caused significant reductions of H3K27me3 enrichment in both *VEGF-A* distal and proximal promoter regions, and siHOTAIR treatment reversed such reductions (Supplementary Figs. S20B, E). Moreover, when compared to NG controls, HG augmented the enrichment of H3K9/14/18/23/27 acetylation in both *VEGF-A* promoter regions, and knockdown of *HOTAIR* prevented glucose-induced increases in pan-acetylation levels (Supplementary Figs. S20C, F). Hence, a dynamic interplay exists among *HOTAIR*, histone-modifying enzymes, and RNA polymerase II in the transcriptional regulation of *VEGF-A* in hyperglycemia.

### **Glucose Does Not Cause Duration-Dependent CpG Methylation Alterations in HOTAIR**

To investigate DNA methylation, we performed a genome-wide DNA methylation analysis following incubation of HRECs in NG or HG for 2 and 7 days. Following the detection of >860,000 CpG sites/probes, we interrogated CpG sites that spanned the *HOTAIR* gene (5 kb upstream to 1 kb downstream, corresponding to 59 probes). The average methylation intensity was lower for the majority of the probes ( $\beta < 0.3$ ), except for seven probes for which the methylation intensities were greater ( $0.2 < \beta < 0.5$ ; corresponding to north/south shelf and north/south shore regions) (Fig. 7). A stable DNA methylation pattern persisted in all

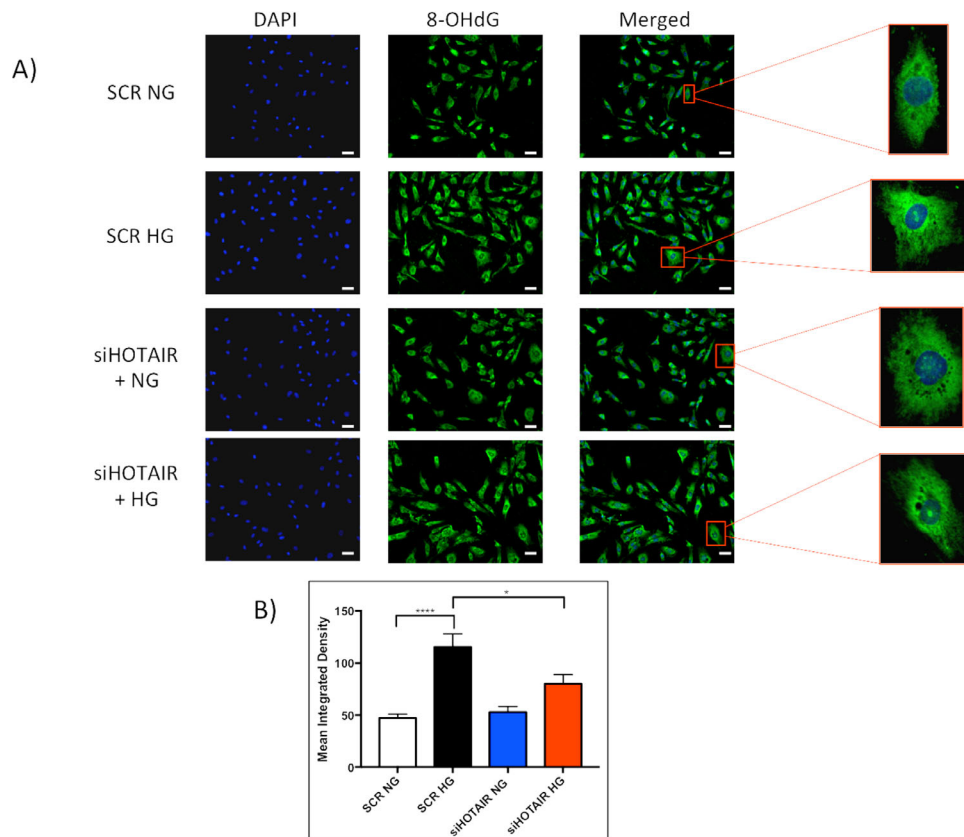


**FIGURE 6.** Knockdown of *HOTAIR* significantly prevents glucose-induced oxidative damage. **(A)** Images captured from the 8-OHdG assay, where HRECs were pretreated with SCR siRNAs or siHOTAIR and subsequently cultured in NG or HG for 48 hours. 8-OHdG stains showed that HG-induced nuclear and mitochondrial oxidative DNA damage (indicated by stronger green fluorescence) was prevented by siHOTAIR. Cells were also counterstained with DAPI. Original magnification, 20 $\times$ . Scale bars: 100  $\mu$ m. **(B)** Mean integrated densities of 8-OHdG expression were quantified using ImageJ. Statistical significance was assessed using one-way ANOVA for multiple comparisons, followed by Tukey's post hoc test (\* $P < 0.05$ , \*\*\*\* $P < 0.0001$ ). Data represent the mean  $\pm$  SEM of 20 cells captured per sample ( $n = 8$  independent samples per group).

groups across the *HOTAIR* genomic region (Supplementary Fig. S21A). HRECs in HG also displayed a slight trend toward a reduction of DNA methylation in the *HOTAIR* promoter compared to NG (Supplementary Fig. S21B). These findings suggest stable epigenetic DNA methylation across *HOTAIR* in HRECs during hyperglycemia.<sup>16</sup>

### DNA Methyltransferases Differentially Regulate *HOTAIR* and Some of Its Targets

To examine the cause-and-effect relationship of DNA methylation on the expression of *HOTAIR* and its targets, we used 5-aza-2'-deoxycytidine (5-aza-dC; a demethylating agent). Following 5-aza-dC administration, *DNMT1*, *DNMT3A*, and *DNMT3B* RNA levels were reduced compared to HG (Supplementary Figs. S22A–C). Simultaneously, we observed elevations of *HOTAIR*, *ET-1*, *CTCF*, *cytochrome b*, *MCP-1*, *IL-1 $\beta$* , *HOXD3*, and *HOXD10* transcripts, whereas no significant differences were observed for *ANGPTL4*, *P300*, or *PARP1* expression (Supplementary Figs. S22, S23). In keeping with previous observations,<sup>31</sup> global inhibition of DNA methyltransferases prevented glucose-induced increases in *VEGF-A* mRNA (Supplementary Fig. S23B).

To confirm these findings, we silenced the constitutively expressed *DNMT1*. Accompanying a  $\sim$ 71% knock-

down following siDNMT1 transfection in HG-cultured cells (Supplementary Fig. S24), *DNMT3A* and *DNMT3B* transcripts were significantly reduced. In parallel, significant increases in RNA expression were observed for *HOTAIR*, *ET-1*, *CTCF*, *cytochrome b*, *PARP1*, *IL-1 $\beta$* , *HOXD3*, and *HOXD10* following *DNMT1* knockdown in HG (Supplementary Figs. S24, S25). Although no differences were observed for *ANGPTL4*, *P300*, or *MCP-1* after such knockdown, significant reductions in *VEGF-A* transcripts still remained in siDNMT1-transfected HRECs in HG (Supplementary Fig. S25B), confirming the observations from 5-aza-dC experiments. It is possible that depending on the genomic location, inhibition of DNA methylation has varying effects on distal or intragenic regulatory elements with different degrees of CpG density, subsequently regulating gene expression.<sup>32</sup>

### DISCUSSION

Angiogenesis is critical for vascular homeostasis.<sup>2,33</sup> In DR, hyperglycemia promotes increased permeability and angiogenesis, which leads to vision-threatening complications.<sup>2</sup> Although angiogenesis and DME are primarily mediated by VEGF-A,<sup>2,34</sup> limitations in current anti-VEGF therapies suggest that our understanding of the pathobiology of DR remains incomplete. Deciphering novel molecular mediators may allow for the development of biomarkers and better



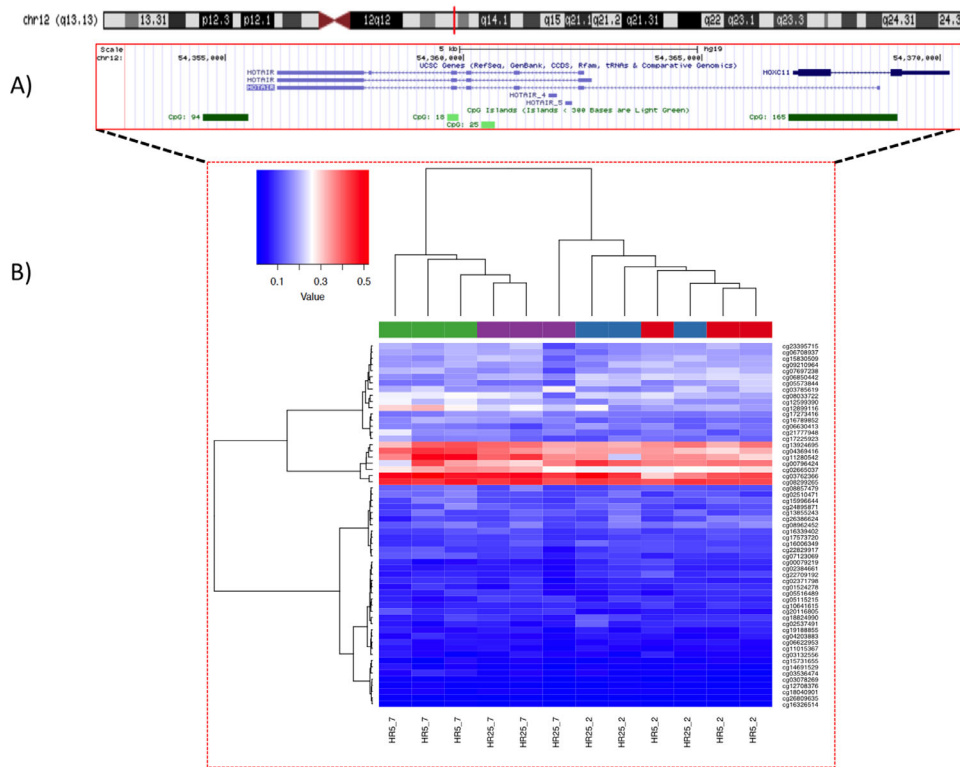


**FIGURE 7.** DNA methylation profiling of HRECs. **(A)** Human *HOTAIR* is located on chromosome 12:54,356,092–54,368,740 (hg19), and its approximate size (for transcript variant 1) is 12,649 nucleotides containing a total of six exons (UCSC database<sup>54</sup>). **(B)** Unsupervised hierarchical clustering with heatmap using all the CpGs in HRECs that span across *HOTAIR*, which amounted to 59 probes. No distinctions were noted between cells treated with different concentrations of glucose (5 mM vs. 25 mM) or the duration of culture (2 vs. 7 days). Rows indicate CpGs and columns show the samples; the color scale from blue to red indicates the level of methylation from 0 to 1 (with 0 indicating no methylation and 1 indicating maximum methylation) ( $n = 3$  independent samples per group, indicated by the top panel colors). HR5\_2, HRECs cultured in 5-mM glucose for 2 days; HR25\_2, HRECs cultured in 25-mM glucose for 2 days; HR5\_7, HRECs cultured in 5-mM glucose for 7 days; HR25\_7, HRECs cultured in 25-mM glucose for 7 days.

targeted therapies. Recently, lncRNAs have garnered attention due to their critical regulatory capabilities in several diseases; however, very few lncRNAs have been comprehensively characterized.

Here, we provide evidence that the lncRNA *HOTAIR* mediates angiogenesis and other pathologic changes in DR through complex epigenetic mechanisms (Fig. 8). Targeted knockdown of *HOTAIR* showed that siHOTAIR can protect against glucose-induced increases of several angiogenic factors, diabetes-associated molecules, and epigenetic mediators. *HOTAIR* contributes to glucose-induced mitochondrial and DNA damage and facilitates the epigenetic activation of *VEGF-A* by recruiting RNA polymerase II and acetylators (P300) to the *VEGF-A* promoter, causing VEGF-A overexpression and angiogenesis. Furthermore, *HOTAIR* and its target molecules are differentially regulated through histone and DNA methyltransferases and transcription factors.

Similar to mRNAs, lncRNAs exhibit a wide range of stability profiles where lncRNA half-lives correlate with genomic location, splicing, GC percentage, and subcellular localization.<sup>35</sup> The lncRNAs that are spliced, localized in the cytoplasm, classified as intergenic or cis-antisense, or contain high GC percentage are considered to be more stable than those lncRNAs that are unspliced, classified as intronic, or nuclear retained or that contain a low GC percentage. The degree of stability is critical for lncRNA function, as nuclear-residing lncRNAs with short half-lives have rapid turnover

that contributes to the dynamic processes they regulate.<sup>35,36</sup> Interestingly, cell-specific variations exist for the half-life of *HOTAIR*.<sup>37</sup> Here, we found significant glucose-induced elevations of *HOTAIR* at 48 hours. Our results are in keeping with similar expression patterns observed for another lncRNA, *MALAT1*, in HRECs,<sup>14</sup> suggesting that lncRNAs may have distinct and overlapping expression profiles. Furthermore, based on previous reports,<sup>38</sup> it may be plausible that initial glucose-induced *HOTAIR* expression may activate persisting epigenetic changes and gene expression.

As noted above, the subcellular localization of lncRNAs provides insights into their functions. Cytoplasmic lncRNAs cause post-transcriptional modifications governing mRNA stability and translation, whereas nuclear-retained lncRNAs are involved in transcriptional regulation, organization of nuclear architecture, and alternative splicing.<sup>39,40</sup> Certain lncRNAs can also be found in both nucleus and cytoplasm, where they shape the epigenome, regulate organelle formation and function, and influence transcription and translation.<sup>39,40</sup> In keeping with previous findings,<sup>41</sup> we showed that *HOTAIR* is present in both nuclear and cytoplasmic compartments of ECs. It is possible that *HOTAIR* regulates the expression of several transcripts while simultaneously targeting enzymes involved in histone modification and DNA methylation. For example, *HOTAIR* depletion in fibroblasts causes loss of *HOXD* silencing and H3K27me3 by PRC2,<sup>26</sup> whereas *HOTAIR* overexpression promotes cellular

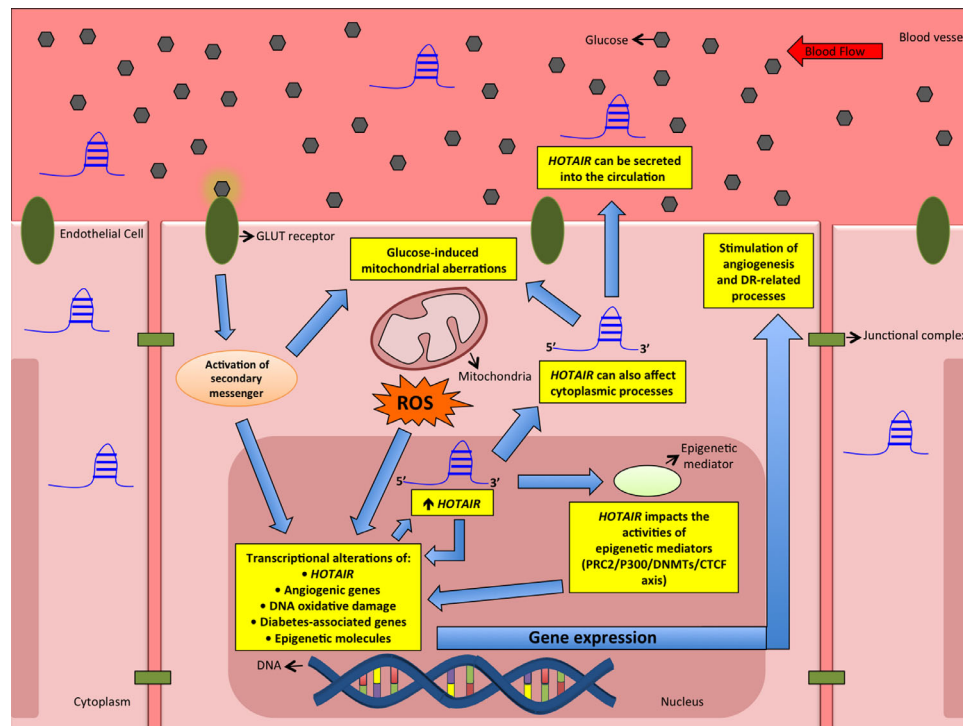


**FIGURE 8.** Schematic of hyperglycemia-induced regulation of lncRNA *HOTAIR* in retinal endothelial cells. *HOTAIR* can regulate the transcription of several genes implicated in the pathogenesis of diabetic retinopathy through direct and indirect mechanisms involving alterations in the PRC2–P300–DNMT–CTCF epigenetic axis. *HOTAIR* can also contribute to both mitochondrial and DNA oxidative damage. ROS, reactive oxygen species.

invasiveness through selective retargeting of PRC2 and H3K27me3, enabling the expression of invasion-related genes.<sup>42</sup> In the context of DR, a recent study has also reported that *HOTAIR* can bind to lysine-specific histone demethylase 1 and subsequently inhibit VE-cadherin transcription by reducing H3K4me3 levels on its promoter, which further facilitates *HIF-1 $\alpha$* -mediated transcriptional activation of *VEGF-A*.<sup>43</sup> Hence, *HOTAIR* may function as a molecular scaffold to regulate gene expression through interactions with epigenetic mediators in DR.<sup>20</sup>

We demonstrated that *HOTAIR* contributes to glucose-induced mitochondrial and oxidative DNA damage in ECs. Other studies have shown that *HOTAIR* can mediate DNA damage response through the regulation of NF- $\kappa$ B activation<sup>44</sup> and maintain mitochondrial function,<sup>22</sup> where *HOTAIR* knockdown results in the dysregulation of several proteins associated with mitochondrial function in HeLA cells.<sup>22</sup> We observed that *HOTAIR* knockdown protects the mitochondria. Although cell-specific regulations may exist for *HOTAIR*, our results could be attributed to stress-induced mechanisms involving mitophagy and autophagy. For example, hyperglycemia evokes oxidative stress, membrane depolarization, and mitochondrial fragmentation.<sup>2,45</sup> Increases in reduced cytochrome b and specific mitophagy factors (including autophagy-related genes, *ATG11* and *ATG32*) can then trigger non-specific autophagy.<sup>46</sup> A recent study has also demonstrated that *HOTAIR* promotes autophagy by upregulating *ATG7*.<sup>47</sup>

Microvasculature aberrations represent one of the earliest pathological manifestations of DR. Hyperglycemia compromises the function and integrity of the endothelium, leading to increased permeability. Coupled with retinal capil-

lary non-perfusion, endothelium damage and activation of several biochemical pathways further stimulate production of inflammatory cytokines and vasoactive factors.<sup>2,4</sup> We have shown both in vitro and in vivo that a large number of these molecules are *HOTAIR* dependent, and our findings are in keeping with a recent study that confirmed the direct implications of *HOTAIR* in retinal EC dysfunction and increased permeability.<sup>43</sup> Similar data have also been reported in some malignancies, where *HOTAIR* promotes angiogenesis in nasopharyngeal carcinoma via direct and indirect mechanisms (involving glucose regulated protein 78) that activate the transcription of *VEGF-A* and angiotensin-2.<sup>48</sup> Additionally, another study reported that *HOTAIR* affects angiogenesis by regulating *VEGF-A* expression in glioma cells and can be transmitted into endothelial cells through glioma cell-derived extracellular vesicles.<sup>49</sup> The knockdown of *HOTAIR* can also restrict proliferation and invasion of retinoblastoma cells via the Notch signaling pathway.<sup>50</sup> Given our findings, we recognize the limitations that only male animals were used in the experiments and that other non-retinal endothelial cell types may have been possibly targeted following siHOTAIR administration. Moreover, as we planned to avoid additional confounding variables by maintaining diabetic animals without external insulin, we were unable to assess advanced retinal microangiopathy such as acellular capillaries in our short-term animal model. We further noted that *HOTAIR* blockade, although increasing cell survival, prevented tube formation; thus, it is tempting to speculate that a differential effect of *HOTAIR* on cellular proliferation and differentiation may be responsible in DR. However, such hypotheses should be validated by additional experiments.

With *HOTAIR* demonstrating potential involvement in DR, we addressed the clinical utility of *HOTAIR* as a biomarker. Compared to non-diabetic controls, *HOTAIR* levels were significantly upregulated in the VH and serum of PDR patients. These results are in keeping with our previously published findings for another lncRNA, *MALAT1*, in DR.<sup>14</sup> The demonstrated correlations in *HOTAIR* RNA levels between serum and VH of PDR patients raises the possibility of using *HOTAIR* as a potential biomarker for DR. Our data are in keeping with another study that alludes to the diagnostic and prognostic roles of *HOTAIR* in DR.<sup>51</sup>

Furthermore, with regard to its potential as a therapeutic, targeting *HOTAIR* in DR may offer significant advantages over existing anti-VEGF compounds (protein-based), as RNA-based drugs have shown to silence target genes with high efficiency and specificity. They are chemically synthesized without the variability of biologics and exhibit low immunogenicity, and chemically modified siRNAs can even persist for many months in humans, suggesting that RNA therapeutics could be administered less frequently.<sup>52,53</sup> Undoubtedly, additional experimentation is warranted to further validate the pharmacokinetic profile, clinical durability, and cell specificity of siHOTAIR in DR, as well as its impact on various VEGF isoforms.

In summary, this report demonstrates that the lncRNA *HOTAIR* critically mediates angiogenesis in DR by directly regulating the expression of multiple DR-associated molecules through a complex epigenetic axis. *HOTAIR* also has implications in glucose-induced oxidative mitochondrial and DNA damage, and *HOTAIR* expression in the VH and serum correlates with PDR. Collectively, this study has identified the potential for *HOTAIR* to serve as a diagnostic and therapeutic target in DR.

### Acknowledgments

The authors thank Linda Jackson-Boeters and David Malott for their technical expertise, as well as Martin Duennwald, PhD, for providing access to instrumentation. SCha is the guarantor of this work and, as such, had full access to all of the data in the study and takes responsibility for the integrity of the data and accuracy of the data analysis.

Supported and funded by the Canadian Institutes of Health Research.

Disclosure: **S. Biswas**, None; **B. Feng**, None; **S. Chen**, None; **J. Liu**, None; **E. Aref-Eshghi**, None; **J. Gonder**, None; **V. Ngo**, None; **B. Sadikovic**, None; **S. Chakrabarti**, None

### References

1. Cho NH, Shaw JE, Karuranga S, et al. IDF Diabetes Atlas: global estimates of diabetes prevalence for 2017 and projections for 2045. *Diabetes Res Clin Pract.* 2018;138:271–281.
2. Biswas S, Chakrabarti S. Pathogenetic mechanisms in diabetic retinopathy: from molecules to cells to tissues. In: Kartha CC, Ramachandran S, Pillai RM, eds. *Mechanisms of Vascular Defects in Diabetes Mellitus*. Cham: Springer; 2017:209–247.
3. Nentwich MM, Ulbig MW. Diabetic retinopathy – ocular complications of diabetes mellitus. *World J Diabetes.* 2015;6(3):489–499.
4. Grant MB, Afzal A, Spoerri P, Pan H, Shaw LC, Mames RN. The role of growth factors in the pathogenesis of diabetic

- retinopathy. *Expert Opin Investig Drugs.* 2004;13(10):1275–1293.
5. Levy AP, Levy NS, Wegner S, Goldberg MA. Transcriptional regulation of the rat vascular endothelial growth factor gene by hypoxia. *J Biol Chem.* 1995;270(22):13333–13340.
6. Wang Y, Zang QS, Liu Z, et al. Regulation of VEGF-induced endothelial cell migration by mitochondrial reactive oxygen species. *Am J Physiol Cell Physiol.* 2011;301(3):695–704.
7. Angelo LS, Kurzrock R. Vascular endothelial growth factor and its relationship to inflammatory mediators. *Clin Cancer Res.* 2007;13(10):2825–2830.
8. Ruiz MA, Feng B, Chakrabarti S. Polycomb repressive complex 2 regulates MiR-200b in retinal endothelial cells: potential relevance in diabetic retinopathy. *PLoS One.* 2015;10(4):e0123987.
9. Thomas AA, Biswas S, Chakrabarti S. ANRIL: a regulator of VEGF in diabetic retinopathy. *Invest Ophthalmol Vis Sci.* 2017;58(1):470–480.
10. Van Wijngaarden P, Coster DJ, Williams KA (2005). Inhibitors of ocular neovascularization: promises and potential problems. *JAMA.* 2005;293(12):1509–1513.
11. Duh EJ, Sun JK, Stitt AW. Diabetic retinopathy: current understanding, mechanisms, and treatment strategies. *JCI Insight.* 2017;2(14):e93751.
12. Wang D, Fu P, Yao C, et al. Long non-coding RNAs, novel culprits, or bodyguards in neurodegenerative diseases. *Mol Ther Nucleic Acids.* 2018;10:269–276.
13. Thomas AA, Biswas S, Feng B, Chen S, Gonder J, Chakrabarti S. lncRNA H19 prevents endothelial–mesenchymal transition in diabetic retinopathy. *Diabetologia.* 2019;62(3):517–530.
14. Biswas S, Thomas AA, Chen S, et al. MALAT1: an epigenetic regulator of inflammation in diabetic retinopathy. *Sci Rep.* 2018;8(1):6526.
15. Liu J, Chen S, Biswas S, et al. Glucose-induced oxidative stress and accelerated aging in endothelial cells are mediated by the depletion of mitochondrial SIRT6. *Physiol Rep.* 2020;8(3):e14331.
16. Aref-Eshghi E, Biswas S, Chen C, Sadikovic B, Chakrabarti S. Glucose-induced duration-dependent genome-wide DNA methylation changes in human endothelial cells. *Am J Physiol Cell Physiol.* 2020;319(2):C268–C276.
17. Turchinovich A, Zoidl G, Dermietzel R. Non-viral siRNA delivery into the mouse retina in vivo. *BMC Ophthalmol.* 2010;10(1):25.
18. Qazi Y, Maddala S, Ambati BK. Mediators of ocular angiogenesis. *J Genet.* 2009;88(4):495–515.
19. Pacher P, Szabó C. Role of poly(ADP-ribose) polymerase-1 activation in the pathogenesis of diabetic complications: endothelial dysfunction, as a common underlying theme. *Antioxid Redox Signal.* 2005;7(11-12):1568–1580.
20. Li L, Liu B, Wapinski OL, et al. Targeted disruption of *HOTAIR* leads to homeotic transformation and gene derepression. *Cell Rep.* 2013;5(1):3–12.
21. DeCicco-Skinner KL, Henry GH, Cataisson C, et al. Endothelial cell tube formation assay for the in vitro study of angiogenesis. *J Vis Exp.* 2014;(91):e51312.
22. Zheng P, Xiong Q, Wu Y, et al. Quantitative proteomics analysis reveals novel insights into mechanisms of action of long noncoding RNA Hox transcript antisense intergenic RNA (*HOTAIR*) in HeLa cells. *Mol Cell Proteomics.* 2015;14(6):1447–1463.
23. Aft RL, Zhang FW, Gius D. Evaluation of 2-deoxy-D-glucose as a chemotherapeutic agent: mechanism of cell death. *Br J Cancer.* 2002;87(7):805–812.
24. Hoffmann S, Spitkovsky D, Radicella JP, Epe B, Wiesner RJ. Reactive oxygen species derived from the mitochondrial



- respiratory chain are not responsible for the basal levels of oxidative base modifications observed in nuclear DNA of mammalian cells. *Free Radic Biol Med.* 2004;36(6):765–773.
25. Merchan JR, Kovács K, Railsback JW, et al. Antiangiogenic activity of 2-deoxy-D-glucose. *PLoS One.* 2010;5(10):e13699.
  26. Rinn JL, Kertesz M, Wang JK, et al. Functional demarcation of active and silent chromatin domains in human HOX loci by noncoding RNAs. *Cell.* 2007;129(7):1311–1323.
  27. Miranda TB, Cortez CC, Yoo CB, et al. DZNep is a global histone methylation inhibitor that reactivates developmental genes not silenced by DNA methylation. *Mol Cancer Ther.* 2009;8(6):1579–1588.
  28. Tan JZ, Yan Y, Wang XX, Jiang Y, Xu HE. EZH2: biology, disease, and structure-based drug discovery. *Acta Pharmacol Sin.* 2014;35(2):161–174.
  29. Hajjari M, Rahnema S. HOTAIR long non-coding RNA: characterizing the locus features by the in silico approaches. *Genomics Inform.* 2017;15(4):170–177.
  30. Ong CT, Corces VG. Modulation of CTCF insulator function by transcription of a noncoding RNA. *Dev Cell.* 2008;15(4):489–490.
  31. Xie MY, Yang Y, Liu P, Luo Y, Tang SB. 5-aza-2'-deoxycytidine in the regulation of antioxidant enzymes in retinal endothelial cells and rat diabetic retina. *Int J Ophthalmol.* 2019;12(1):1–7
  32. Wan J, Oliver VF, Wang G, et al. Characterization of tissue-specific differential DNA methylation suggests distinct modes of positive and negative gene expression regulation. *BMC Genomics.* 2015;16(1):49.
  33. Potente M, Gerhardt H, Carmeliet P. Basic and therapeutic aspects of angiogenesis. *Cell.* 2011;146(6):873–887.
  34. Shibuya M. Vascular endothelial growth factor (VEGF) and its receptor (VEGFR) signaling in angiogenesis. *Genes Cancer.* 2011;2(12):1097–1105.
  35. Clark MB, Johnston RL, Inostroza-Ponta M, et al. Genome-wide analysis of long noncoding RNA stability. *Genome Res.* 2012;22(5):885–898.
  36. Dinger ME, Amaral PP, Mercer TR, Mattick JS. Pervasive transcription of the eukaryotic genome: functional indices and conceptual implications. *Brief Funct Genomic Proteomic.* 2009;8(6):407–423.
  37. Yoon JH, Abdelmohsen K, Kim J, et al. Scaffold function of long non-coding RNA HOTAIR in protein ubiquitination. *Nat Commun.* 2013;4:2939.
  38. El-Osta A, Brasacchio D, Yao D, et al. Transient high glucose causes persistent epigenetic changes and altered gene expression during subsequent normoglycemia. *J Exp Med.* 2008;205(10):2409–2417.
  39. Lai F, Orom UA, Cesaroni M, et al. Activating RNAs associate with Mediator to enhance chromatin architecture and transcription. *Nature.* 2013;494(7438):497–501.
  40. Krause HM. New and prospective roles for lncRNAs in organelle formation and function. *Trends Genet.* 2018;34(10):736–745.
  41. Yu GJ, Sun Y, Zhang DW, Zhang P. Long non-coding RNA HOTAIR functions as a competitive endogenous RNA to regulate PRAF2 expression by sponging miR-326 in cutaneous squamous cell carcinoma. *Cancer Cell Int.* 2019;19(1):270.
  42. Gupta RA, Shah N, Wang KC, et al. Long non-coding RNA HOTAIR reprograms chromatin state to promote cancer metastasis. *Nature.* 2010;464(7291):1071–1076.
  43. Zhao D, et al. Long noncoding RNA HOTAIR facilitates retinal endothelial cell dysfunction in diabetic retinopathy. *Clin Sci (Lond).* 2020;134(17):2419–2434.
  44. Özeş AR, Miller DF, Özeş ON, et al. NF-κB-HOTAIR axis links DNA damage response, chemoresistance and cellular senescence in ovarian cancer. *Oncogene.* 2016;35(41):5350–5361.
  45. Devi TS, Somayajulu M, Kowluru RA, Singh LP. TXNIP regulates mitophagy in retinal Müller cells under high-glucose conditions: implications for diabetic retinopathy. *Cell Death Dis.* 2017;8(5):e2777.
  46. Deffieu M, Kiššová I, Salin B, et al. Increased levels of reduced cytochrome *b* and mitophagy components are required to trigger nonspecific autophagy following induced mitochondrial dysfunction. *J Cell Sci.* 2013;126(2):415–426.
  47. Wu C, Yang L, Qi X, Wang T, Li M, Xu K. Inhibition of long non-coding RNA HOTAIR enhances radiosensitivity via regulating autophagy in pancreatic cancer. *Cancer Manag Res.* 2018;10:5261–5271.
  48. Fu W-M, Lu Y-F, Hu B-G, et al. Long noncoding RNA HOTAIR mediated angiogenesis in nasopharyngeal carcinoma by direct and indirect signaling pathways. *Oncotarget.* 2016;7(4):4712–4723.
  49. Ma X, Li Z, Li T, Zhu L, Li Z, Tian N. Long non-coding RNA HOTAIR enhances angiogenesis by induction of VEGFA expression in glioma cells and transmission to endothelial cells via glioma cell derived-extracellular vesicles. *AM J Transl Res.* 2017;9(11):5012–5021.
  50. Dong C, Liu S, Lv Y, et al. Long non-coding RNA HOTAIR regulates proliferation and invasion via activating Notch signalling pathway in retinoblastoma. *J Biosci.* 2016;41(4):677–687.
  51. Shaker OG, Abdelaleem OO, Mahmoud RH, et al. Diagnostic and prognostic role of serum miR-20b, miR-17-3p, HOTAIR, and MALAT1 in diabetic retinopathy. *IUBMB Life.* 2019;71(3):310–320.
  52. Fitzgerald K, White S, Borodovsky A, et al. A highly durable RNAi therapeutic inhibitor of PCSK9. *N Engl J Med.* 2017;376(1):41–51.
  53. Lieberman J. Tapping the RNA world for therapeutics. *Nat Struct Mol Biol.* 2018;25(5):357–364.
  54. Kent WJ, Sugnet CW, Furey TS, et al. The human genome browser at UCSC. *Genome Res.* 2002;12(6):996–1006.
  55. Kungulovski G, Nunna S, Thomas M, Zanger UM, Reinhardt R, Jeltsch A. Targeted epigenome editing of an endogenous locus with chromatin modifiers is not stably maintained. *Epigenetics Chromatin.* 2015;8(1):12.
  56. Chen S, Apostolova MD, Cherio MG, Chakrabarti S. Interaction of endothelin-1 with vasoactive factors in mediating glucose-induced increased permeability in endothelial cells. *Lab Invest.* 2000;80(8):1311–1321.